


Enaminone-based carboxylic acids as novel non-classical carbonic anhydrases inhibitors: design, synthesis and *in vitro* biological assessment

Mahmoud F. Abo-Ashour^a, Hadia Almahli^b, Alessandro Bonardia^c, Amira Khalil^d, Tarfah Al-Warhi^e, Sara T. Al-Rashood^f, Hatem A. Abdel-Aziz^g, Alessio Nocentini^c , Claudiu T. Supuran^c  and Wagdy M. Eldehna^h

^aDepartment of Pharmaceutical Chemistry, Faculty of Pharmacy, El saleheya El Gadida University, Cambridge, Egypt; ^bDepartment of Chemistry, University of Cambridge, Cambridge, United Kingdom; ^cDepartment of NEUROFARBA, Section of Pharmaceutical and Nutraceutical Sciences, University of Florence, Firenze, Italy; ^dPharmaceutical Chemistry Department, Faculty of Pharmacy, The British University in Egypt (BUE), Cairo, Egypt; ^eDepartment of Chemistry, College of Science, Princess Nourah Bint Abdulrahman University, Riyadh, Saudi Arabia; ^fDepartment of Pharmaceutical Chemistry, College of Pharmacy, King Saud University, Riyadh, Saudi Arabia; ^gDepartment of Applied Organic Chemistry, National Research Center, Dokki, Egypt; ^hDepartment of Pharmaceutical Chemistry, Faculty of Pharmacy, Kafrelsheikh University, Kafrelsheikh, Egypt

ABSTRACT

In searching for new molecular drug targets, Carbonic Anhydrases (CAs) have emerged as valuable targets in diverse diseases. CAs play critical functions in maintaining pH and CO₂ homeostasis, metabolic pathways, and much more. So, it is becoming attractive for medicinal chemists to design novel inhibitors for this class of enzymes with improved potency and selectivity towards the different isoforms. In the present study, three sets of carboxylic acid derivatives **5a–q**, **7a–b** and **12a–c** were designed, developed and evaluated for the hCA inhibitory effects against hCA I, II, IX and XII. Compounds **5l**, **5m**, and **5q** elicited the highest inhibitory activities against hCA II, IX and XII. In summary, structural rigidification, regioisomerism and structural extension, all played obvious roles in the degree of hCA inhibition. This present work could be a good starting point for the design of more non-classical selective hCA inhibitors as potential targets for several diseases.

ARTICLE HISTORY

Received 26 June 2022
Revised 11 August 2022
Accepted 13 August 2022

KEYWORDS

Carbonic anhydrase; H-NMR; enaminone; stopped-flow assay

1. Introduction

The Zn(II) metalloenzymes carbonic anhydrases (CA, EC 4.2.1.1) is a very significant family in humans and in most living organisms that catalyses the reversible CO₂ hydration reaction to bicarbonate ion¹. This fundamental reaction orchestrates several physiological processes requiring pH control and ion transport². Fifteen humans (*h*) CA isoforms have been discovered so far, and they showed diverse distribution among tissues and cells.





Dysfunction of *h*CA activities results in several pathological consequences, highlighting these isozymes as promising drug targets for diverse therapeutic interventions with small molecule CA inhibitors (CAIs)³. Accordingly, the pharmacological applications of several CAIs were reported for the management of different diseases including ophthalmologic problems^{4,5}, human malignancies⁶, high-altitude sickness⁷, epilepsy⁸, peptic ulcers⁹, obesity¹⁰, and congestive heart failure¹¹.


Carbonic anhydrases are classically inhibited by small molecules tethered with the primary sulphonamide-based zinc binding group (ZBG), as well as its bioisosteres such as sulfamides and sulfamates^{12–14}. Although several chemotypes of CA inhibitors have been identified in the last few decades (such as coumarins, phenols, thiocarbamates, and carboxylates)^{15–17} only CA inhibitors based on sulphonamides could be used in the clinical setting for

glaucoma treatment (such as acetazolamide, methazolamide and dorzolamide, Figure 1), and in clinical trials for the treatment of human malignancies (such as SLC-0111 and indisulam, Figure 1)^{18,19}. Accordingly, the development of non classical CA inhibitors has emerged as a promising approach to discovering new efficient CA inhibitors for the management of various disorders.

The carboxylic acid-bearing small molecules represent an important category of the non-classical carbonic anhydrase inhibitors²⁰. Interestingly, they can inhibit the metalloenzymes *via* various modes of action. Firstly, they are able to bind directly to the catalytic zinc displacing bound water-hydroxide anion, similarly to sulphonamides. Alternatively, certain carboxylic acid derivatives can anchor to the zinc-bound water-hydroxide ion *via* a hydrogen bonding, similar to the binding mode noticed for phenol-based molecules. Lastly, carboxylates may bind within an adjacent pocket to the entrance which is located outside the active site of the carbonic anhydrase. This interaction results in a block of the proton shuttle His64 residue in its “out” conformation, leading to the inhibition of CA catalytic activity^{21–23}.

In 2020, our research team has reported novel series of benzofuran-based carboxylic acid small molecules that tethered with benzoic or hippuric acid motifs as potential CA inhibitors²⁴.

CONTACT Wagdy M. Eldehna  wagdy2000@gmail.com  Department of Pharmaceutical Chemistry, Faculty of Pharmacy, Kafrelsheikh University, P.O. Box 33516, Kafrelsheikh, Egypt; Claudiu T. Supuran  claudiu.supuran@unifi.it  Department of NEUROFARBA, Section of Pharmaceutical and Nutraceutical Sciences, University of Florence, Polo Scientifico, Via U. Schiff 6, Firenze, Sesto Fiorentino, 50019, Italy

 Supplemental data for this article can be accessed online at <https://doi.org/10.1080/14756366.2022.2114079>.

© 2022 The Author(s). Published by Informa UK Limited, trading as Taylor & Francis Group.

This is an Open Access article distributed under the terms of the Creative Commons Attribution License (<http://creativecommons.org/licenses/by/4.0/>), which permits unrestricted use, distribution, and reproduction in any medium, provided the original work is properly cited.

These acid moieties are linked to 5-bromobenzofuran or 2-methylbenzofuran tail through an ureido linker. Among these acid derivatives, *m*-benzoic acid-bearing derivative (Compound **1**, Figure 2) emerged as submicromolar *h*CA IX inhibitor ($K_i = 0.79 \mu\text{M}$), as well as potent *h*CAXII inhibitor ($K_i = 2.3 \mu\text{M}$). Moreover, we developed another ureides series of piperine-based carboxylic acid derivatives that incorporate benzoic acid moieties linked to the natural product piperine through an ureido spacer²⁵. Acid derivative **2** (Figure 2) exerted moderate inhibition activities against both CA IX and XII isoforms ($K_i = 16.1 \mu\text{M}$ and $14.4 \mu\text{M}$, respectively).

Also, in 2020 we designed and prepared a novel methylthiazolo[3,2-*a*]benzimidazole-tethered carboxylic acid derivatives as potential CA inhibitors²⁶. In this work, the enaminone linker was utilised to link the ZBG benzoic acid motifs to the thiazolo[3,2-*a*]benzimidazole tail²⁶. Enaminone-based carboxylic acid **3** (Figure 2) effectively inhibited *h*CA IX and XII isoforms ($K_i = 0.83 \mu\text{M}$ and

$2.4 \mu\text{M}$, respectively). In the current work, we devoted our effort to developing new non-classical CA inhibitors through the design of three sets of new carboxylic acid derivatives (**5a-q**, **7a-b** and **12a-c**), Figure 3.

The first (**5a-q**) and the second (**7a-b**) sets incorporated a benzoic acid moiety that is connected to different aryl tails through an enaminone linker, for the first set, or through the more flexible saturated 3-oxo-propylamine linker, for the second set, Figure 3. The incorporation of the enaminone linker is expected to provide more rigid molecules, than the corresponding molecules that tethered with the 3-oxo-propylamine linker. The expected conformational restriction in the enaminone-bearing carboxylic acids (**5a-q**) should be attributed to the unsaturation (the olefinic functional group), as well as due to the formation of an intramolecular hydrogen bonding that resulted in a pseudo-six-membered ring. Lastly, a structural extension approach was utilised to replace the benzoic acid motif with the hippuric acid to furnish the third series **12a-c** (Figure 3). The potential ability of the target carboxylic acids (**5a-q**, **7a-b** and **12a-c**) to inhibit *h*CA I, II, IX and XII isoforms was assessed *via* the stopped-flow carbon dioxide hydrase assay.

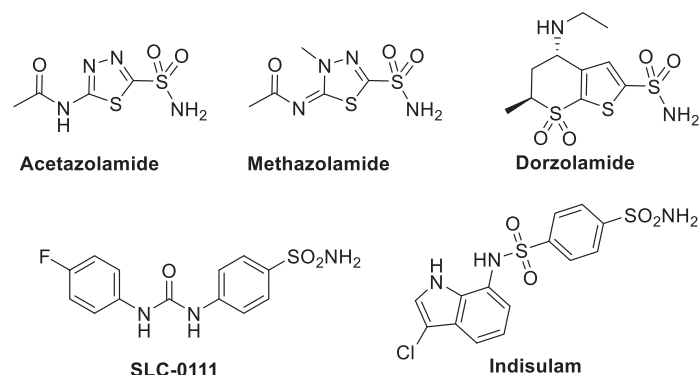


Figure 1. Structures of certain sulphonamide-based CAIs in clinical use and in clinical trials.

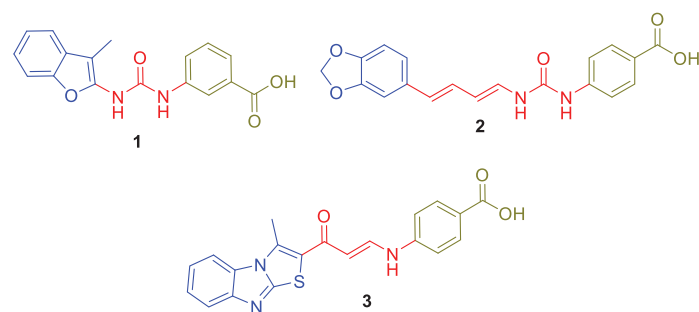


Figure 2. Structures for some reported carboxylic acid derivatives as non-classical CA inhibitors.

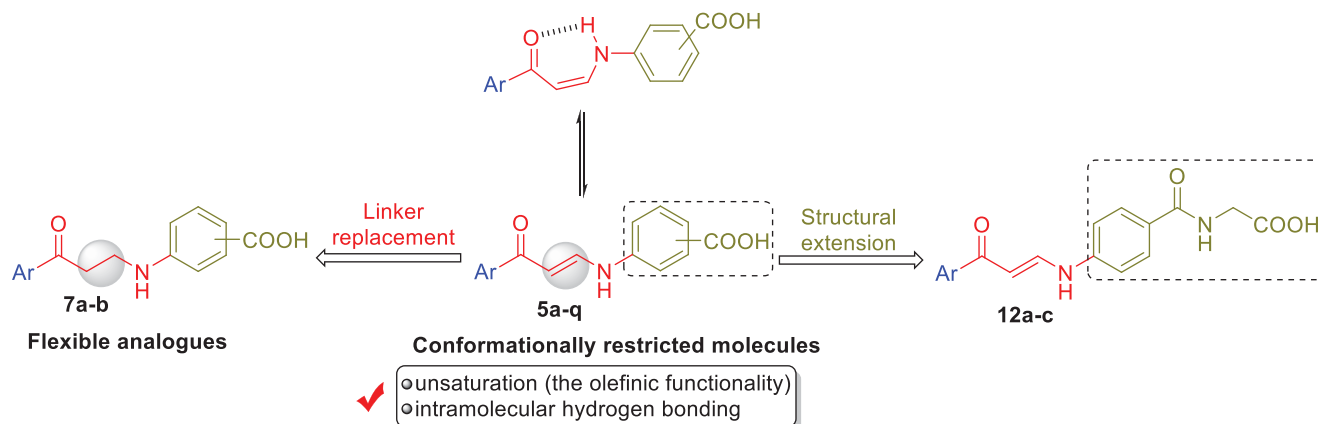


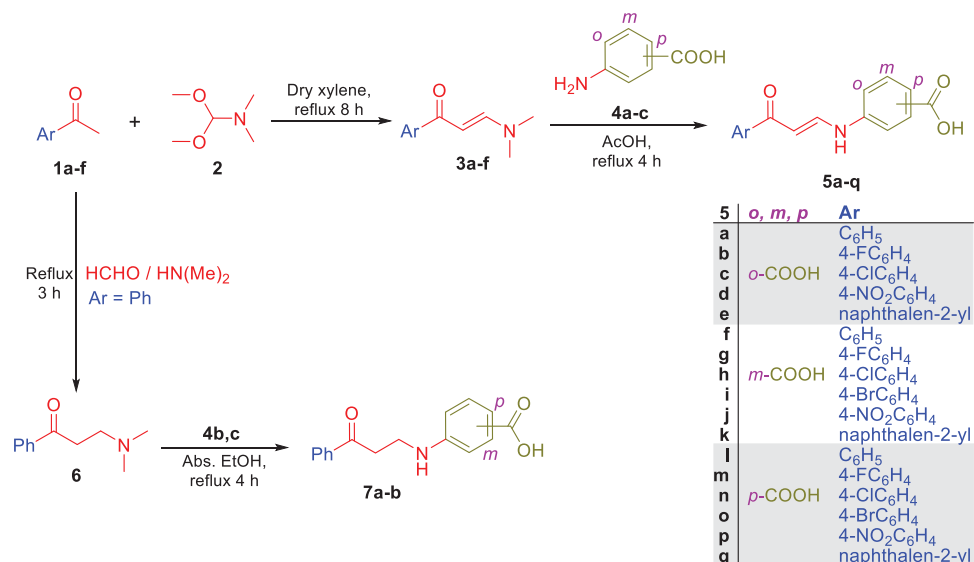
Figure 3. Design for herein reported carboxylic acid derivatives **5a-q**, **7a-b** and **12a-c**.

2. Results and discussion

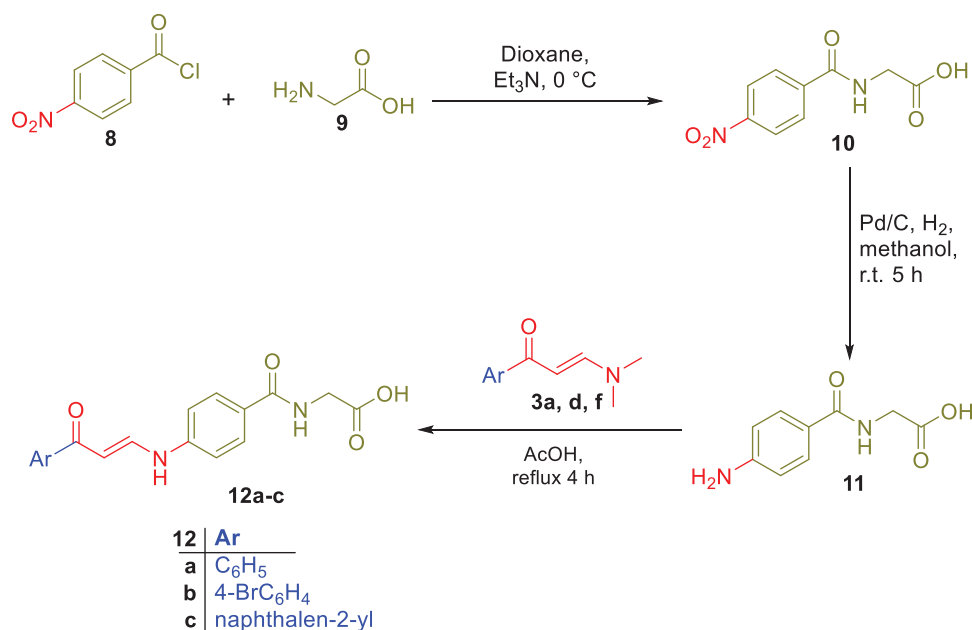
2.1. Chemistry

In this study, the synthesis of the new carboxylic acids-based carbonic anhydrase inhibitors **5a-q**, **7a-b** and **12a-c** is outlined in Schemes 1 and 2. In Scheme 1, six aryl methyl ketones **1a-f** were condensed with DMF-DMA to furnish the corresponding aryl enaminones intermediates **3a-f** that subsequently reacted with *ortho*, *meta* and *para* aminobenzoic acids **4a-c** in glacial acetic acid to produce the target carboxylic acids **5a-q**. On the other hand, acetophenone **1a** has been reacted with dimethyl amine and formaldehyde *via* Mannich reaction to get 3-(dimethylamino)-1-phenylpropan-1-one **6**, which subsequently reacted with *m*- and *p*-aminobenzoic acids **4b-c** in absolute ethanol to furnish targeted carboxylic acids **7a-b** with saturated linker between the ZBG and the aryl tail.

In Scheme 2, glycine **9** was acylated with 4-nitrobenzoyl chloride **8** in dry dioxan to get (4-nitrobenzoyl)glycine **10**, which was then reduced to the corresponding (4-aminobenzoyl)glycine **11**. The third set of the target carboxylic acids with the desired structural extension **12a-c** was prepared through the nucleophilic substitution reaction of (4-aminobenzoyl)glycine **11** with the previously prepared enaminones **3a,d,f** in a boiling glacial acetic acid



Scheme 1. Synthesis of benzoic acids-bearing enamionones **5a–q** and 3/4-((3-oxo-3-phenylpropyl)amino)benzoic acids **7a–b**.



Scheme 2. Synthesis of hippuric acids-bearing enamionones **12a–c**.

(Scheme 2). The proposed structure for carboxylic acids enamionones **5a–q**, **7a–b** and **12a–c** were supported by the elemental and spectral data.

¹H NMR spectra of 2-substituted carboxylic acids bearing enamionones **5a–e** revealed they are existing in *Z*-form around the olefinic bond which was evidenced by up-field doublets of *Z*-H_a around δ 6.13–6.37 ppm with coupling constant (*J*) equals 8.0 Hz. The latter *Z*-form was assumed to be established through the formation of two intramolecular hydrogen bonds that resulted in two pseudo-six-membered rings. ¹H NMR spectra of *ortho*-carboxylic acids bearing enamionones **5a–e** exhibited a doublet D₂O exchangeable signal that was integrated for one proton, attributable to the NH group of the *Z*-form, at more down-field region δ 13.2–13.7 ppm when compared with those of 3- and 4-substituted carboxylic acids bearing enamionones **5f–k** and **5l–q**, respectively, at δ 11.5–12.1 ppm (Figure 4). This negative shift could be explained by the presence of the two intramolecular hydrogen

bonds. The coupling constant value of these doublets is 12.0 Hz which suggests the *trans* direction of NH around HN-CH_b in enamionones **5a–e**.

¹H NMR spectra of 3- and 4-substituted carboxylic enamionones **5f–k** and **5l–q** disclosed their presence in *Z/E* geometric conjugation around H_aC=CH_b in an equal ratio (*Z:E* = 1:1) according to the integrations of their signals. The presence of *E*-isomer was evidenced via the *J* constant for olefinic protons H_a and H_b (*J*_{H_a-H_b} = 12.00 Hz) which was determined by the down-field doublet signal of *E*-H_a around δ 6.4–6.7 ppm (Figures 4 and 5). In a similar way, the presence of the *Z*-form was revealed by determining the *J* constant for the olefinic protons H_a and H_b (*J* = 8.0 Hz) that came from the up-field doublet signals of *Z*-H_a around δ 6.13–6.41 ppm. Furthermore, the ¹H NMR spectra displayed 2 doublet signal sets, integrated for one proton, each belonging to the (NH) proton for the *E* and *Z* isomers around δ 10.28–10.59 and 12.03–12.14 ppm (Figures 4 and 5).

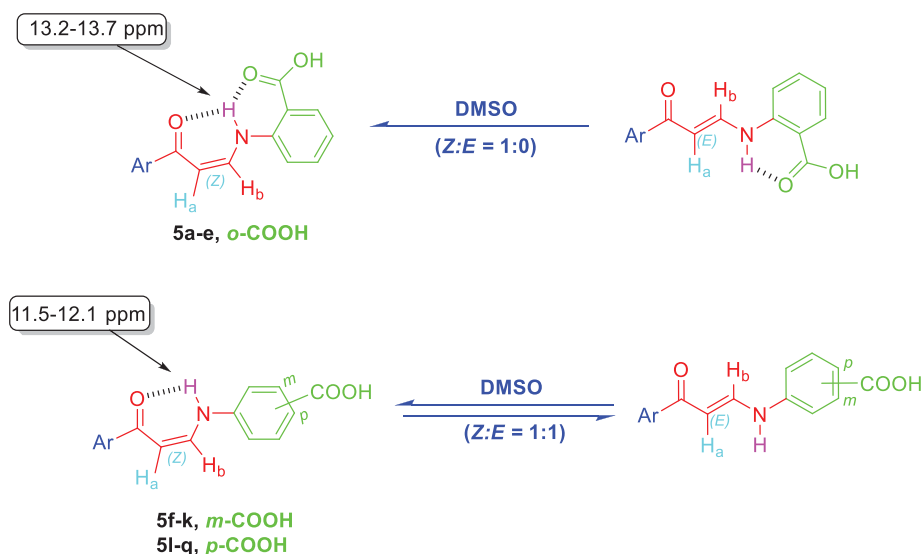


Figure 4. The existence of *ortho*-substituted carboxylic acids enaminones **5a–e** in *Z*-form and the existence of *meta*- and *para*-substituted carboxylic acids enaminones **5f–k** and **5l–q** in *E/Z*-forms (1:1) in DMSO.

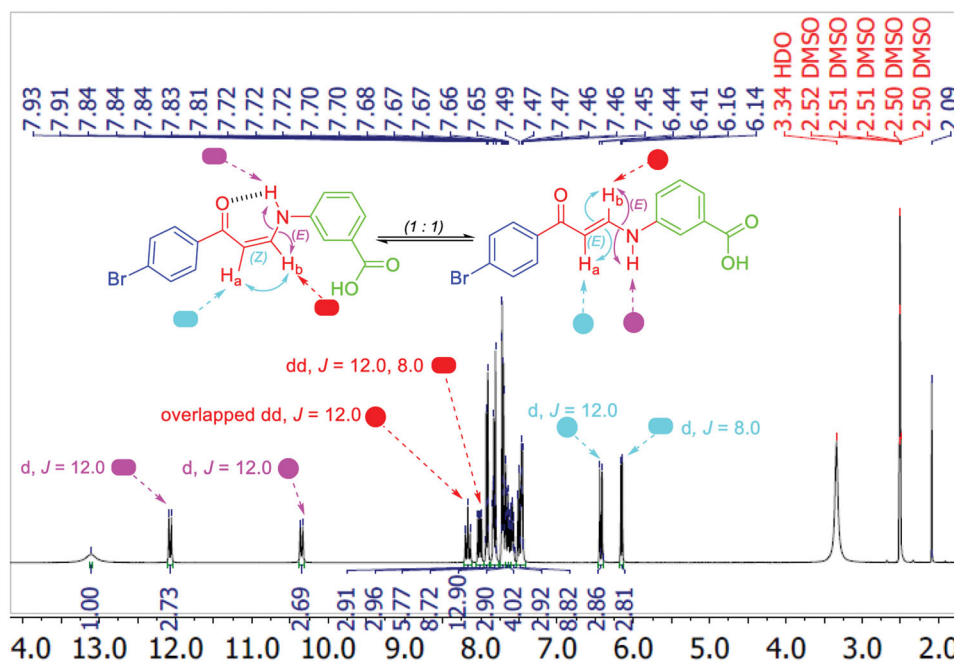


Figure 5. ^1H NMR of enaminone **5i** showing the presence of *Z*-form [*Z* H_a (d), *Z* H_b (dd), *E* NH (d)] and *E*-form [*E* H_a (d), *E* H_b (overlapped dd), *E* NH (d)] in DMSO as a representative example for enaminones **5f–k** and **5l–q**.

The downfield signals of NH proton could be attributed to the *Z* isomer and the up-field signals for the same group to the *E* isomer according to their integration values as explained in our previous study²⁷. The coupling constants for these doublets are 12.0 Hz which suggests the presence of NH of enaminones **5f–k** and **5l–q** in *trans* direction for H_b around HN-CH_b bond in both forms *E* and *Z* (Figures 4 and 5). Moreover, *Z* (NH) appeared down-field, due to the formation of intra-molecular hydrogen bonding with the carbonyl oxygen. However, this hydrogen bond between C=O and NH groups was absolutely confirmed, in a previous study, by X-ray single crystal analysis of a sulphonamide analog for compound **5** which exhibited a *Z* configuration around $\text{H}_a\text{C}=\text{CH}_b$ with the *trans* HN-CH_b ²⁷.

Interestingly, the ^1H NMR of *meta*-substituted carboxylic enaminones **5g** and **5i**, as well as ^1H NMR for *para*-substituted

carboxylic enaminones **5o**, among **5f–k** and **5l–q**, revealed the appearance of down-field *Z*- H_b signal around δ 8.00 ppm as dd with $J = 12.0$ and 8.0 Hz due to $J_{E-\text{H}_b-\text{NH}}$ and $J_{Z-\text{H}_b-\text{H}_a}$, respectively, whereas the up-field *E*- H_b signal appeared around δ 8.14 as overlapped dd with two $J = 12.0$ Hz ($J_{E-\text{H}_b-\text{NH}} = J_{E-\text{H}_b-\text{H}_a} = 12.0$ Hz). It is worthy to note that after the addition of D_2O to the DMSO solution of these compounds (**5g**, **5i** and **5o**) in their NMR tube, the coupling of NH proton for H_b in both *Z* and *E* forms disappeared and the dd of *Z*- H_b was converted to doublet signal due to the coupling of *Z*- H_a only with $J = 8.0$ Hz parallel with the conversion of overlapped dd of *E*- H_b to doublet signal due to *E*- H_a coupling only with $J = 12.0$ Hz (Figure 6).

Furthermore, the ^1H NMR of 4-carboxamido enaminone **12b**, as a representative example for enaminones **12a–c**, showed the appearance of two sets of doublet signals, integrated for the two

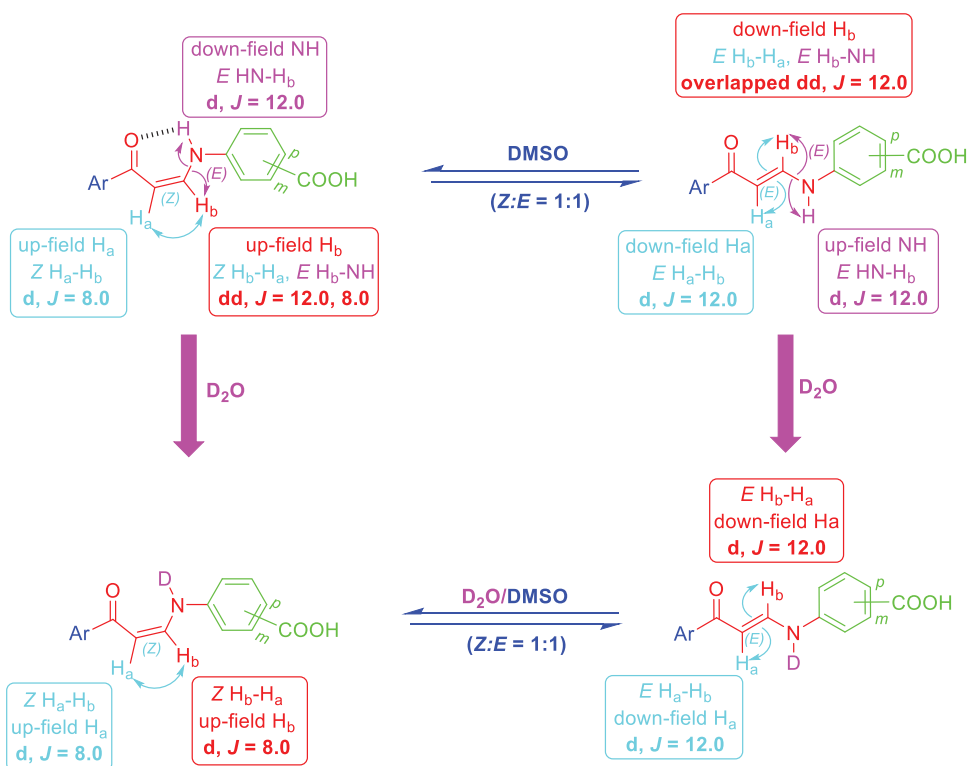


Figure 6. The presence of *meta*- and *para*-substituted carboxylic enaminones 5f–k and 5l–q in Z/E-forms in DMSO and in $\text{D}_2\text{O}/\text{DMSO}$ (^1H NMR).

protons of $-\text{CH}_2-$ at δ 3.91 and δ 3.92 and two sets of triplet, for the proton of the amidic $-\text{NH}$ group of at δ 8.74 and δ 8.79 beside two sets of doublet Z/E H_a and Z/E, H_b , and two dd of E NH, Figure 7.

2.2. Biological evaluation

2.2.1. CAS inhibition

In the current study, we have explored the inhibitory activities of the synthesised carboxylic acid derivatives 5a–q, 7a–b and 12a–c against different carbonic anhydrase isoforms (I, II, IX and XII) using acetazolamide (AAZ) as a reference CA inhibitor. The resulted inhibition constants were presented in Table 1.

The stopped-flow assay outputs disclosed that the off-target cytosolic *hCA* I exhibited the lowest inhibition in this study. Both the ortho and meta carboxylic acids bearing enaminones (5a–e and 5f–k) didn't exert any noticeable inhibitory activity towards this isoform ($K_i > 100 \mu\text{M}$), whereas the para carboxylic acids bearing enaminones 5l, 5m, 5n, 5p and 5q exhibited weak inhibitory effect ($K_i = 75.3, 68.8, 81.5, 95.6$ and $79.4 \mu\text{M}$, respectively), Table 1. In like manner, the target carboxylic acids 7a–b with a saturated 3-oxo-propylamine linker showed the same behaviour; the meta carboxylic acid derivative 7a emerged as inactive, whereas the para carboxylic acid derivative 7b emerged as a weak inhibitor for the *hCA* I isoform ($K_i = 63.8 \mu\text{M}$), Table 1.

Moreover, the stopped-flow assay outputs showed that the physiologically relevant *hCA* II isoform was affected by herein reported carboxylic acids bearing enaminones 5a–q and carboxylic acids 7a–b. Both the ortho and meta carboxylic acids bearing enaminones (5a–e and 5f–k) moderately inhibited *hCA* II isoform with inhibition constants spanning in the ranges 24.3–49.0 μM and 68.2–92.3 μM , respectively, whereas the para carboxylic acids bearing enaminones 5l–q effectively inhibited this isoform (K_i range: 7.4–15.3 μM). In addition, carboxylic acids 7a–b with a saturated

3-oxo-propylamine linker displayed K_i values equal to 64.3 μM and 16.7 μM , respectively. In particular, the best inhibitory activity in the CO_2 hydrase assay was demonstrated by the para carboxylic acids bearing enaminones 5l, 5m and 5q that showed K_i values in the single-digit micromolar range equal to 9.8 μM , 8.7 μM and 7.4 μM , respectively. Also, carboxylic acids 5n, 5o, 5p and 7b exhibited good activity against *hCA* II isoform with $K_i = 13.5 \mu\text{M}$, 15.3 μM , 12.6 μM and 16.7 μM , respectively.

Regarding the effect of the regioisomerism with the enaminones series 5a–q, it was found that shifting the carboxylic acid group from the ortho position (compounds 5a–e) to the meta position (compounds 5f–k) resulted in decreasing activity. For example, the phenyl and naphthyl-bearing enaminones 5f and 5k displayed about 2-fold decreased potency ($K_i = 72.8 \mu\text{M}$ and 92.3 μM , respectively), in comparison to their ortho counterparts 5a and 5e ($K_i = 39.4 \mu\text{M}$ and 49.0 μM , respectively), Table 1. In turn, shifting the carboxylic acid functionality from the ortho position (enaminones 5a–e) to the para position (enaminones 5l–q) led to about 2–6.5 fold enhancement of the inhibitory activity against *hCA* II isoform. For example, the phenyl and naphthyl-bearing enaminones 5l and 5q emerged as more potent inhibitors ($K_i = 9.8 \mu\text{M}$ and 7.4 μM , respectively) than their ortho analogues 5a and 5e ($K_i = 39.4 \mu\text{M}$ and 49.0 μM , respectively). Similarly in the second set, the para carboxylic acid derivative 7b displayed better activity ($K_i = 16.7 \mu\text{M}$) than its meta counterpart 7a ($K_i = 64.3 \mu\text{M}$) against *hCA* II isoform, Table 1.

The trans-membrane *hCA* IX, the third examined isoform, was effectively inhibited by all carboxylic acids bearing enaminones 5a–q and carboxylic acids 7a–b evaluated here, with inhibition constants spanning in the range 0.76–32.5 μM . The best inhibitory action towards *hCA* IX isoform has been observed for enaminones 5m and 5q with sub-micromolar inhibition constants (0.92 μM and 0.76 μM , respectively), whereas compounds 5g, 5l, 5n, 5o, 5p and 7b exerted good inhibitory activity with K_i s in the single-digit

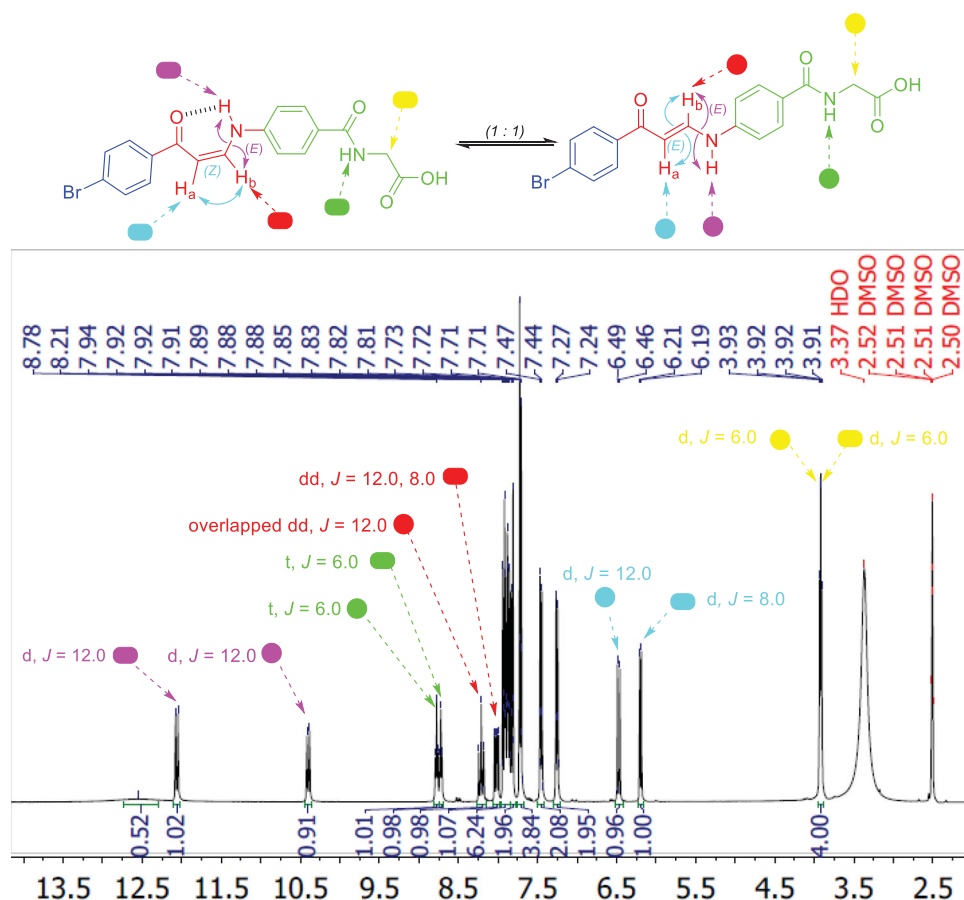


Figure 7. ^1H NMR of enaminone **12b** which showed the existence of *Z*- and *E*-form in DMSO as a representative example for **12a-c**.

Table 1. hCA I, II, IX and XII inhibition results from the carboxylic acid derivatives **5a-q**, **7a-b** and **12a-c** and acetazolamide (AAZ) as a reference CA inhibitor.

Cmpd.	COOH	Ar	K_i (μM) ^a			
			hCA I	hCA II	hCA IX	hCA XII
5a	<i>ortho</i>	-C ₆ H ₅	>100	39.4	10.6	6.4
5b	<i>ortho</i>	-4-F-C ₆ H ₄	>100	24.3	13.2	4.3
5c	<i>ortho</i>	-4-Cl-C ₆ H ₄	>100	32.7	17.7	12.5
5d	<i>ortho</i>	-4-NO ₂ -C ₆ H ₄	>100	26.9	14.1	7.8
5e	<i>ortho</i>	-2-Naph	>100	49.0	19.3	15.7
5f	<i>meta</i>	-C ₆ H ₅	>100	72.8	15.9	9.5
5g	<i>meta</i>	-4-F-C ₆ H ₄	>100	68.2	9.6	10.3
5h	<i>meta</i>	-4-Cl-C ₆ H ₄	>100	77.1	19.2	8.6
5i	<i>meta</i>	-4-Br-C ₆ H ₄	>100	81.4	32.5	13.9
5j	<i>meta</i>	-4-NO ₂ -C ₆ H ₄	>100	80.7	24.7	8.9
5k	<i>meta</i>	-2-Naph	>100	92.3	11.4	9.7
5l	<i>para</i>	-C ₆ H ₅	75.3	9.8	1.2	0.97
5m	<i>para</i>	-4-F-C ₆ H ₄	68.8	8.7	0.92	1.1
5n	<i>para</i>	-4-Cl-C ₆ H ₄	81.5	13.5	3.4	4.6
5o	<i>para</i>	-4-Br-C ₆ H ₄	>100	15.3	5.6	6.2
5p	<i>para</i>	-4-NO ₂ -C ₆ H ₄	95.6	12.6	4.1	0.85
5q	<i>para</i>	-2-Naph	79.4	7.4	0.76	1.5
7a	<i>meta</i>	-C ₆ H ₅	>100	64.3	23.7	7.4
7b	<i>para</i>	-C ₆ H ₅	63.8	16.7	8.3	9.1
12a	-	-C ₆ H ₅	>100	>100	>100	>100
12b	-	-4-Br-C ₆ H ₄	>100	>100	>100	>100
12c	-	-2-Naph	>100	>100	>100	>100
AAZ	-	-	0.250	0.012	0.025	0.006

^aMean from 3 different assays (errors were in the range of \pm 5–10% of the reported values).

micromolar range equal to 9.6 μM , 1.2 μM , 3.4 μM , 5.6 μM , 4.1 μM and 8.3 μM , respectively.

As discussed above for the inhibitory activity against *hCA* II, grafting the carboxylic acid functionality at the para position (enaminones **5l–q**) resulted in a much-enhanced activity (K_i range: 0.76–5.6 μM) in comparison to the ortho (enaminones **5a–e**; K_i range: 10.6–19.3 μM) and meta (enaminones **5f–k**; K_i range: 11.4–32.5 μM) counterparts, Table 1. For example, the phenyl and naphthyl-bearing enaminones **5l** and **5q** showed about 9- and 25-fold enhanced potency ($K_i = 1.2 \mu\text{M}$ and 0.76 μM , respectively) in comparison to their ortho counterparts **5a** and **5e** ($K_i = 10.6 \mu\text{M}$ and 19.3 μM , respectively), and showed about 13- and 15-fold increased activity in comparison to their meta counterparts **5f** and **5k** ($K_i = 15.9 \mu\text{M}$ and 11.4 μM , respectively). In like manner, the para carboxylic acid derivative **7b** exerted better *hCA* IX inhibitory activity ($K_i = 8.3 \mu\text{M}$) than its meta counterpart **7a** ($K_i = 23.7 \mu\text{M}$), Table 1.

On the other hand, examining the impact of the substitution of the phenyl tail within the most potent enaminones series (**5l–q**) revealed that only grafting the small fluorine substituent (enaminone **5m**; $K_i = 0.92 \mu\text{M}$) can enhance the activity of the unsubstituted phenyl-bearing enaminone **5l** ($K_i = 0.92 \mu\text{M}$). In turn, substituting the phenyl tail with 4-Cl, 4-Br or 4-NO₂ substituents reduced the activity. Moreover, the replacement of the phenyl tail with a naphthyl one resulted in the most potent *hCA* IX inhibitor in this work (enaminone **5m**; $K_i = 0.76 \mu\text{M}$), Table 1. Notably, the same SAR could be observed for the ortho carboxylic acids bearing enaminones **5f–k**.

It is worthy to mention that the phenyl-bearing enaminones **5f** and **5l** exhibited better activity against *hCA* IX ($K_i = 15.9 \mu\text{M}$ and 1.2 μM , respectively) than their flexible counterparts **7a–b** that bear the saturated 3-oxo-propylamine linker ($K_i = 23.7 \mu\text{M}$ and 8.3 μM , respectively) which hints out that the conformational restriction for herein reported compounds is more favourable for *hCA* IX inhibitory action.

The newly reported carboxylic acids (**5a–q** and **7a–b**) efficiently inhibited the trans-membrane *hCA* XII isoform with K_i range of 0.85–15.7 μM . Uniquely, the para carboxylic acids bearing enaminones **5l** and **5p** induced inhibition in the submicromolar range, with K_i s of 0.97 μM and 0.85 μM , respectively. Similarly, to the inhibition profile for both *hCA* II and IX isoforms, the para carboxylic acids bearing enaminones (**5l–q**) exerted more potent activity (K_i range: 0.85–6.2 μM) than their ortho (enaminones **5a–e**; K_i range: 4.3–15.7 μM) and meta (enaminones **5f–k**; K_i range: 8.6–13.9 μM) counterparts, Table 1. With an exception for the 4-NO₂ substitution (enaminone **5p**; $K_i = 0.85 \mu\text{M}$), neither substitution of the phenyl tail nor its bioisosteric replacement with the naphthyl moiety enhanced the *hCA* XII inhibitory activity.

Finally, the third set of hippuric acid-bearing enaminones **12a–c** couldn't inhibit any of the examined CA isoforms up to 100 μM , highlighting that the structural extension approach is not appropriate for the CA inhibitory activity (Table 1).

3. Conclusion

Three sets of our designed non-classical CA inhibitors (**5a–q**, **7a–b** and **12a–c**) were synthesised and evaluated for their CA inhibitory activity. The first (**5a–q**) and the second (**7a–b**) sets incorporated a benzoic acid moiety that is connected to different aryl tails through an enaminone linker, for the first set, or through the more flexible saturated 3-oxo-propylamine linker, for the second set. For the third set, a structural extension approach was utilised to replace the benzoic acid motif with the hippuric acid to furnish

the carboxylic acid derivatives **12a–c**. The inhibitory activity for the prepared carboxylic acids was variable across the four tested CA isoforms, where for example, most compounds showed no or weak inhibition towards *hCA* I. Furthermore, compounds **5q**, **5m**, and **5l** exhibited a very similar inhibition pattern towards *hCA* II and IX with K_i values equal to 7.4, 8.7, 9.8 and 0.76, 0.92, 1.2 μM respectively. Regarding *hCA* XII, the para nitro-substituted derivative **5p** showed the highest inhibitory activity. Structural extension as done in the third set **12a–c**, showed no inhibitory actions towards all tested *hCA* isoforms, which suggested that this extension might lead to undesired interactions within the CA active site. Generally, ortho/meta carboxylic acid substituted derivatives exhibited weaker inhibitory activities against the tested *hCAs*. Future studies could reveal the desired pharmacophoric features which could enhance *hCA* inhibitory actions, as well as selectivity across different isoforms, that belong to this family of enzymes.

4. Experimental

4.1. Chemistry

4.1.1. General

Stuart melting point apparatus was used for melting point measurements and were uncorrected. Shimadzu FT-IR 8400S spectrophotometer was used to record Infra-red (IR) spectra as KBr discs. NMR Spectra were recorded on a Bruker NMR spectrometer, at 400 and 100 MHz for ¹H spectrum and ¹³C spectrum, respectively, and were run at 100 MHz in deuterated dimethylsulphoxide (DMSO-*d*₆). HRMS spectra were recorded by a Bruker MicroTOF spectrometer.

4.1.2. Synthesis of intermediates 3, 6 and 10

3-(Dimethylamino)-1-phenylprop-2-en-1-ones (**3a–f**²⁸) 3-(dimethylamino)-1-phenylpropan-1-one (**6**²⁹) and (4-aminobenzoyl)glycine (**11**³⁰) were prepared according to the literature procedures.

4.1.3. Synthesis of the target carboxylic acids enaminones 5a–q

An amount of 0.6 mmol from the appropriate enaminone intermediate **3a–f** was dissolved in 4 ml glacial acetic acid, then the required amount (0.8 g, 0.6 mmol) of *o*-, *m*-, *p*-aminobenzoic acid **4a–c** was added to the reaction mixture. Reflux was continued for 3 h, and then the precipitated solid was filtered off while hot, washed with hot 70% ethanol (3 × 2 ml), dried and recrystallized from DMF/methanol mixture (1:4) to yield the target enaminones **5a–q** (Supporting Information).

4.1.4. Synthesis of target 3/4-((3-oxo-3-phenylpropyl)amino)benzoic acids 7a–b

To a hot solution of 3-(dimethylamino)-1-phenylpropan-1-one **6** (0.25 g, 1.41 mmol) in absolute ethanol (12 ml), an equivalent amount of *m*- or *p*-aminobenzoic acid **4b–c** (0.19 g, 1.41 mmol) was added, and the mixture was heated under reflux for 4 h. The formed solid, after cooling, was collected and washed with aq. potassium bicarbonate solution and cold methanol (2 × 3 ml), then recrystallized from isopropanol to get the 3/4-((3-oxo-3-phenylpropyl)amino)benzoic acids **7a–b**, respectively (Supporting Information).

4.1.5. Synthesis of target carboxylic acids enamines 12a–c

Enaminones **12a–c** were prepared *via* the same method described previously for enamines **5a–q**, utilising (4-aminobenzoyl)glycine **11** instead of aminobenzoic acids **4a–c** (Supporting Information).

4.2. Biological evaluation

4.2.1. Ca inhibitory assay

The target carbonic anhydrase inhibitors reported in this work were evaluated for their potential CA-catalysed CO₂ hydration activities utilising an Applied Photophysics stopped-flow instrument as described previously^{31–35} (Supporting Materials).

Disclosure statement

CT Supuran is Editor-in-Chief of the Journal of Enzyme Inhibition and Medicinal Chemistry. He was not involved in the assessment, peer review, or decision-making process of this paper. The authors have no relevant affiliations of financial involvement with any organisation or entity with a financial interest in or financial conflict with the subject matter or materials discussed in the manuscript. This includes employment, consultancies, honoraria, stock ownership or options, expert testimony, grants or patents received or pending, or royalties.

Funding

The authors extend their appreciation to the Princess Nourah bint Abdulrahman University Researchers Supporting Project number (PNURSP2022R25), Princess Nourah bint Abdulrahman University, Riyadh, Saudi Arabia. The authors acknowledge financial support from the Researchers Supporting Project number (RSP-2021/103), King Saud University, Riyadh, Saudi Arabia.

ORCID

Alessio Nocentini  <http://orcid.org/0000-0003-3342-702X>
 Claudiu T. Supuran  <http://orcid.org/0000-0003-4262-0323>

References

- Alterio V, Di Fiore A, D'Ambrosio K, et al. Multiple binding modes of inhibitors to carbonic anhydrases: how to design specific drugs targeting 15 different isoforms? *Chem Rev* **2012**;112:4421–68.
- Supuran CT. Advances in structure-based drug discovery of carbonic anhydrase inhibitors. *Expert Opin Drug Discov* **2017**;12:61–88.
- Mishra CB, Tiwari M, Supuran CT. Progress in the development of human carbonic anhydrase inhibitors and their pharmacological applications: where are we today? *Med Res Rev* **2020**;40:2485–565.
- Mincione F, Nocentini A, Supuran CT. Advances in the discovery of novel agents for the treatment of glaucoma. *Expert Opin Drug Discov* **2021**;16:1209–25.
- Supuran CT. Acetazolamide for the treatment of idiopathic intracranial hypertension. *Expert Rev Neurother* **2015**;15:851–6.
- Nerella SG, Singh P, Arifuddin M, Supuran CT. Anticancer carbonic anhydrase inhibitors: a patent and literature update 2018–2022. *Expert Opin Ther Pat* **2022**;32:833–47.
- Swenson ER. Carbonic anhydrase inhibitors and high altitude illnesses. *Subcell Biochem* **2014**;75:361–86.
- Ciccione L, Cerri C, Nencetti S, Orlandini E. Carbonic anhydrase and epilepsy: state of the art and future perspectives. *Molecules* **2021**;26:6380.
- Buzás GM, Supuran CT. The history and rationale of using carbonic anhydrase inhibitors in the treatment of peptic ulcers. In memoriam Ioan Pușcaș (1932–2015). *J Enzyme Inhib Med Chem* **2016**;31:527–33.
- Costa G, Carta F, Ambrosio FA, et al. A computer-assisted discovery of novel potential anti-obesity compounds as selective carbonic anhydrase VA inhibitors. *Eur J Med Chem* **2019**;181:111565.
- Wongboonsin J, Thongprayoon C, Bathini T, et al. Acetazolamide therapy in patients with heart failure: a meta-analysis. *J Clin Med* **2019**;8:349.
- Moi D, Nocentini A, Deplano A, et al. Structure-activity relationship with pyrazoline-based aromatic sulfamates as carbonic anhydrase isoforms I, II, IX and XII inhibitors: synthesis and biological evaluation. *Eur J Med Chem* **2019**;182:111638.
- Bozdag M, Poli G, Angeli A, et al. N-aryl-N'-ureido-O-sulfamates: potent and selective inhibitors of the human carbonic anhydrase VII isoform with neuropathic pain relieving properties. *Bioorg Chem* **2019**;89:103033.
- Zarai S-O, Abduelkarem AR, Anbar HS, et al. Sulfamates in drug design and discovery: pre-clinical and clinical investigations. *Eur J Med Chem* **2019**;179:257–71.
- Al-Warhi T, Sabt A, Elkaeed EB, Eldehna WM. Recent advancements of coumarin-based anticancer agents: an up-to-date review. *Bioorg Chem* **2020**;103:104163.
- Eldeeb AH, Abo-Ashour MF, Angeli A, et al. Novel benzene-sulfonamides aryl and arylsulfone conjugates adopting tail/dual tail approaches: synthesis, carbonic anhydrase inhibitory activity and molecular modeling studies. *Eur J Med Chem* **2021**;221:113486.
- Lomelino CL, Supuran CT, McKenna R. Non-classical inhibition of carbonic anhydrase. *Int J Mol Sci* **2016**;17:1150.
- Masini E, Carta F, Scozzafava A, Supuran CT. Antiglaucoma carbonic anhydrase inhibitors: a patent review. *Expert Opin Ther Pat* **2013**;23:705–16.
- A study of SLC-0111 and gemcitabine for metastatic pancreatic ductal cancer in subjects positive for CAIX (SLC-0111-17-01). [cited 2022 May 30]. Available from: <https://clinicaltrials.gov/ct2/show/NCT03450018>.
- D'Ambrosio K, Carradori S, Monti SM, et al. Out of the active site binding pocket for carbonic anhydrase inhibitors. *Chem Comm* **2015**;51:302–5.
- Supuran CT. How many carbonic anhydrase inhibition mechanisms exist? *J Enzyme Inhib Med Chem* **2016**;31:345–60.
- Supuran CT. Novel carbonic anhydrase inhibitors. *Future Med Chem* **2021**;13:1935–7.
- Cau Y, Vullo D, Mori M, et al. Potent and selective carboxylic acid inhibitors of tumor-associated carbonic anhydrases IX and XII. *Molecules* **2017**;23:17.
- Eldehna WM, Nocentini A, Elsayed ZM, et al. Benzofuran-based carboxylic acids as carbonic anhydrase inhibitors and antiproliferative agents against breast cancer. *ACS Med Chem Letters* **2020**;11:1022–7.
- Elimam DM, Elgazar AA, Bonardi A, et al. Natural inspired piperine-based sulfonamides and carboxylic acids as carbonic anhydrase inhibitors: design, synthesis and biological evaluation. *Eur J Med Chem* **2021**;225:113800.

26. Alkhaldi AA, Al-Sanea MM, Nocentini A, et al. 3-Methylthiazolo [3, 2-a] benzimidazole-benzenesulfonamide conjugates as novel carbonic anhydrase inhibitors endowed with anticancer activity: design, synthesis, biological and molecular modeling studies. *Eur J Med Chem* **2020**;207:112745.
27. Eldehna WM, Abo-Ashour MF, Berrino E, et al. SLC-0111 enaminone analogs, 3/4-(3-aryl-3-oxopropenyl) aminobenzenesulfonamides, as novel selective subnanomolar inhibitors of the tumor-associated carbonic anhydrase isoform IX. *Bioorg Chem* **2019**;83:549–58.
28. Xu R-S, Yue L, Pan Y-J. Regioselective copper(I)-catalyzed C–H hydroxylation/C–S coupling: expedient construction of 2-(styrylthio)phenols. *Tetrahedron* **2012**;68:5046–52.
29. Xu Z, Tice CM, Zhao W, et al. Structure-based design and synthesis of 1,3-oxazinan-2-one inhibitors of 11 β -hydroxysteroid dehydrogenase type 1. *J Med Chem* **2011**;54:6050–62.
30. Glas C, Dietschreit JCB, Wössner N, et al. Identification of the subtype-selective Sirt5 inhibitor balsalazide through systematic SAR analysis and rationalization via theoretical investigations. *Eur J Med Chem* **2020**;206:112676.
31. Abo-Ashour MF, Eldehna WM, Nocentini A, et al. 3-Hydrazinoisatin-based benzenesulfonamides as novel carbonic anhydrase inhibitors endowed with anticancer activity: synthesis, in vitro biological evaluation and in silico insights. *Eur J Med Chem* **2019**;184:111768.
32. Abdelrahman MA, Ibrahim HS, Nocentini A, et al. Novel 3-substituted coumarins as selective human carbonic anhydrase IX and XII inhibitors: synthesis, biological and molecular dynamics analysis. *Eur J Med Chem* **2021**;209:112897.
33. Elimam DM, Eldehna WM, Salem R, et al. Natural inspired ligustrazine-based SLC-0111 analogues as novel carbonic anhydrase inhibitors. *Eur J Med Chem* **2022**;228:114008.
34. Abdelrahman MA, Eldehna WM, Nocentini A, et al. Novel benzofuran-based sulfonamides as selective carbonic anhydrases IX and XII inhibitors: synthesis and in vitro biological evaluation. *J Enzyme Inhib Med Chem* **2020**;35:298–305.
35. Ibrahim HS, Abdelrahman MA, Nocentini A, et al. Insights into the effect of elaborating coumarin-based aryl enamines with sulfonamide or carboxylic acid functionality on carbonic anhydrase inhibitory potency and selectivity. *Bioorg Chem* **2022**;126:105888.